

# bradscholars

## Reverse roll coating with a deformable roll operating at negative gaps

Item Type	Article
Authors	Benkreira, Hadj;Shibata, Yusuke;Ito, K.
Citation	Benkreira H, Shibata Y and Ito K (2017) Reverse roll coating with a deformable roll operating at negative gaps. Chemical Engineering Science. 165: 204-215.
DOI	<a href="https://doi.org/10.1016/j.ces.2017.02.034">https://doi.org/10.1016/j.ces.2017.02.034</a>
Rights	© 2017 Elsevier. Reproduced in accordance with the publisher's self-archiving policy. This manuscript version is made available under the CC-BY-NC-ND 4.0 license ( <a href="https://creativecommons.org/licenses/by-nc-nd/4.0/">https://creativecommons.org/licenses/by-nc-nd/4.0/</a> )
Download date	2026-06-08 01:37:24
Link to Item	<a href="http://hdl.handle.net/10454/11580">http://hdl.handle.net/10454/11580</a>

# The University of Bradford Institutional Repository

<http://bradscholars.brad.ac.uk>

This work is made available online in accordance with publisher policies. Please refer to the repository record for this item and our Policy Document available from the repository home page for further information.

To see the final version of this work please visit the publisher's website. Access to the published online version may require a subscription.

**Link to publisher version:** <http://dx.doi.org/10.1016/j.ces.2017.02.034>

**Citation:** Benkreira H, Shibata Y and Ito K (2017) Reverse roll coating with a deformable roll operating at negative gaps. *Chemical Engineering Science*. 165: 204-215.

**Copyright statement:** © 2017 Elsevier. Reproduced in accordance with the publisher's self-archiving policy. This manuscript version is made available under the [CC-BY-NC-ND 4.0 license](https://creativecommons.org/licenses/by-nc-nd/4.0/).



1                   **REVERSE ROLL COATING WITH A DEFORMABLE ROLL**  
2                   **OPERATING AT NEGATIVE GAPS**

3  
4                   **H. Benkreira<sup>\*,1</sup> and Y. Shibata<sup>\*,‡</sup>, K. Ito<sup>‡</sup>**

5                   <sup>\*</sup>School of Engineering, R&KT Centre in Advanced Materials Engineering  
6                   University of Bradford, BD7 1DP, United Kingdom, UK

7                   <sup>‡</sup>Films R&D Centre, Toyobo Co. Ltd., Otsu, Japan  
8

9                   **ABSTRACT**

10                   Reverse roll coating is probably the most widely used coating operation, yet its full  
11                   potential has not been exploited as it is shown in this paper which considers operation with a  
12                   negative gap. We demonstrate through a wide range of experimental data that such operation  
13                   can yield very thin and stable films with no ribbing or cascade instabilities when low  
14                   viscosity fluids are used. Typically, stable film thickness less than 5 $\mu$ m can be obtained at  
15                   speeds up to 150 m/min when a rubber roller is used at -100  $\mu$ m gap with fluids of viscosity  
16                   in the range 10-200 mPa.s. These film thicknesses can be made to decrease further down to 1  
17                   or 2 microns with a judicious choice of speed ratios (applicator to metering roller) and rubber  
18                   hardness. Such new findings make this simple coating method an attractive roll to roll  
19                   technique for application in the newer coating technologies, such as in the production of solar  
20                   cells and plastic electronics. The data obtained in this study have been underpinned by a  
21                   model based on the classical lubrication theory, well developed for such flow situations.  
22                   Essentially it is shown that the film thickness non dimensionalised with respect to the set  
23                   negative gap is controlled through a single parameter, the elasticity number  $Ne$  which  
24                   combines all the operating parameters. Of course, this flow problem has complexities,  
25                   particularly at high speed ratios and at zero gap so the data obtained here can serve as a basis  
26                   for more comprehensive modelling of this classical fluid mechanic problem.

27  
28                   **Key words:** *reverse roll coating, deformable, negative gap, thin films, cascade, ribbing*  
29

30                   **1. INTRODUCTION**

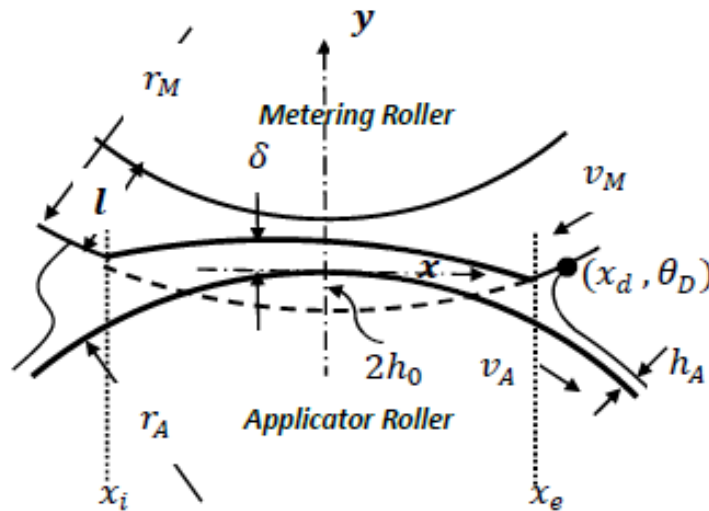
31                   Coating or the deposition of a thin film onto a surface for decorative, protective or  
32                   functional applications is an important industrial operation used to transform paper, textile,  
33                   plastic and metal substrates into highly added value products. Examples are very many and  
34                   include printing paper, letterpress printing plates, photographic films, medical x-rays, audio  
35                   and video magnetic tapes, electronic printed circuits, controlled release medical drug  
36                   substrates, flexible solar panels, membranes and a host of other products. In all these  
37                   applications, the product performance and cost rely critically on how thin, uniform and fast  
38                   the film can be coated. Modern roll to roll production in high-tech applications (plastic  
39                   electronics and photovoltaics for example) require that the coated liquid film be no more than

---

<sup>1</sup> Corresponding author e-mail address: H.Benkreira@bradford.ac.uk

1 a few microns (subsequently drying into nanometers layers) and produced at speed higher  
 2 than 0.5 m/s without any defects such as ribbing which may form on the surface of the film as  
 3 a result of flow instabilities or tiny air bubbles which may be entrained during flow as a result  
 4 of dynamic wetting failure.

5 Of all the coating methods available, roll coating is by far the most used industrially:  
 6 it is economical and simple to organize (two rotating rollers separated by a coating gap fed  
 7 with the coating liquid) and can be operated over large widths (meters). Clearly, as roll  
 8 coating flows are metered by a gap, the lower limit on film thickness is dictated by how small  
 9 a gap the coater can be operated at. In practice, with rigid steel or ceramic rollers, gaps less  
 10 than 25 microns are not used in order to prevent the possibility of the rotating rollers clashing.  
 11 Also as the gaps get smaller, the accuracy of the set gap diminishes because of the roller  
 12 eccentricity which can be up to 25 microns. The end result is that coated films with rigid  
 13 rollers at very low gap settings exhibit significant variations in thickness both in the machine  
 14 and transverse directions. To circumvent these problems and produce thinner films, a  
 15 deformable rubber sleeved roller pressing against a rigid roller system forming a “negative  
 16 gap” is used to create a very small coated film resulting from the elasto-hydrodynamic  
 17 deformation of the rotating rollers. Such a flow situation demands that the rollers rotate  
 18 preferably in the same direction at the nip to prevent possible shearing of the deforming roller.  
 19 Ribbing instabilities are however inevitable in such *forward* roll coating flow (Pearson, 1960;  
 20 Pitts and Greiller, 1961; Benkreira et al., 1982) unless the operation is conducted at very low  
 21 speeds. The quest for a roll coating method that is stable and can be conducted at high speeds  
 22 to produce very thin films leads us in the present work to consider negative gap deformable  
 23 *reverse* roll coating (see Fig. 1).



24

25 **Fig. 1:** Deformable reverse roll coating flow; geometry and pertinent parameters.

26 In this configuration, as the rollers rotate in opposite direction at the nip, the flow that exits  
 27 out of the nip and forms the film will be considerably smaller than in forward roll coating  
 28 particularly when the metering roller to applicator roller speed ratio approaches 1. A  
 29 difficulty with operating negative gap deformable roll coating in the reverse mode is the  
 30 possibility of shearing the deforming roller. However, with good design and control, such a  
 31 problem can be overcome particularly if the method can be proven to deliver the very thin  
 32 film thickness required by the new applications. The aim of this paper is precisely this-to  
 33 assess how thin and uniform the films can be formed by this method and up to what speed.  
 34 An exhaustive literature search has shown only one published work on negative gap reverse

1 deformable roll coating, that of Sasaki et al. (2015) who observed that stability to ribbing was  
 2 expanded when coating fluid viscosity is decreased. They did not however consider the other  
 3 important form of instabilities in reverse roll coating, cascade (further details later), nor did  
 4 they arrive at an operating guide to enable an assessment of how thin uniform films can be  
 5 achieved through this method

## 7 2. THEORETICAL UNDERPINNING

8 Although the literature abounds on the fluid mechanics of rigid and deformable  
 9 forward roll coating and rigid reverse roll coating (see review by Coyle (1997) and the recent  
 10 work of Grashof and Delgado (2015)), there is no published work, experimental or theoretical,  
 11 on negative gap deformable reverse roll coating. As illustrated in Fig. 1, the theoretical  
 12 problem at hand- predicting how the film thickness  $h_A$  varies with operating conditions here  
 13 is a complex one with the flow in the deforming gap  $h$  bounded by a rigid rotating boundary  
 14 (the applicator roller), a deforming rotating boundary (the metering roller), an upstream  
 15 meniscus and a downstream meniscus attached to a dynamic wetting line. The two menisci,  
 16 the deforming boundary and the position  $x_D$  of the dynamic wetting line are all integral parts  
 17 of the solution and in fact the solution of the problem. In principle, a solution to the full 2D  
 18 problem can be found, but whether or not it can grab the entire features of the flow will  
 19 depend on the assumptions made on a number of critical aspects. These include the position  
 20  $x_D$  and contact angle  $\theta_D$  of the dynamic wetting line and how these vary with operating  
 21 conditions: initially applied negative gap  $-2h_0$ , applicator and metering roller speeds  $v_A$   
 22 and  $-v_M$  respectively and coating liquid viscosity  $\mu$  and surface tension  $\sigma$ . There is also the  
 23 question about the type of the deformation  $\delta$  assumed by the rubber sleeve: is it elastic or  
 24 viscoelastic and will it there be shearing of the rubber sleeve as a result of the opposing  
 25 speeds of the applicator and metering rollers? In addition, there is a need to formulate a  
 26 suitable set of pressure boundary conditions, not an easy task for the downstream region  
 27 where the final film forms and a full 2D flow will occur with recirculation as the rollers rotate  
 28 in opposite directions. These issues have been well reviewed by Carvalho and Scriven  
 29 (1997a, b) in their analysis of forward deformable roll coating, the flow of which is more  
 30 unidirectional because the rollers rotate in the same direction at the nip. The flow situation  
 31 with the rollers moving in opposite direction will be comparatively more complex.

32 A simple approach, used extensively in the analysis of roll coating flows, is to apply  
 33 the lubrication approximation, a one dimensional force balance between pressure and viscous  
 34 forces ( $\frac{dp}{dx} = \mu \frac{d^2v}{dy^2}$ ) integrated here with velocity  $v_A$  and  $-v_M$  boundary conditions at the  
 35 rotating walls ( $y_A$  and  $y_M$ ) to relate pressure  $p$  with flow rate per unit width  $q = \int_{y_M}^{y_A} v dy$   
 36 that exits out of the nip to form on the applicator roller a film of thickness  $h_A = q/v_A$ . This  
 37 results with the classical equation describing the pressure drop experienced by the film  
 38 flowing in the coating gap  $h$  :

$$40 \quad \frac{dp}{dx} = 6\mu(v_A - v_M) \left[ \frac{1}{h^2} - \frac{q/\frac{1}{2}(v_A - v_M)}{h^3} \right] \quad (1)$$

41  
 42 Now, in deformable roll coating where a negative gap  $-2h_0$  is initially applied by pressing  
 43 the rubber roller against the steel roller, the coating gap  $h$  that forms is an elasto-  
 44 hydrodynamic gap that is to say it results from the deformation  $\delta(p)$  of the deformable roller

1 caused by the fluid pressure. This deformation must be large enough to offset the negative  
 2 gap for a coating flow to occur. Introducing an equivalent roller radius  $r = 1/\left\{\frac{1}{2}\left(\frac{1}{r_A} + \frac{1}{r_M}\right)\right\}$ , we have from the geometry of Fig.1:

$$3 \quad h = \frac{x^2}{r} + \delta(p) - 2h_0 \quad (2)$$

4  
 5  
 6  
 7 If the rubber sleeve on the metering roller is large enough, then we may assume the  
 8 deformation to be locally of the linear spring type and proportional to pressure:  $\delta(p) =$   
 9  $\frac{1}{k}p = \frac{l}{E}p$  with  $l$  and  $E$  being respectively the thickness and elastic modulus of the rubber  
 10 sleeve. With this simplification which ignores the incompressibility and shear of the rubber  
 11 sleeve and the effect of pressure on deformation of adjoining locations (Carvalho and  
 12 Scriven, 1997a, b), the coating film  $h$  in Eq. (2) will thus be dependent on pressure as:

$$13 \quad h = \frac{x^2}{r} + \frac{l}{E}p - 2h_0 \quad (3)$$

14  
 15  
 16 Eq. (1) becomes then a non-linear differential equation in pressure:

$$17 \quad \frac{dp}{dx} = 6\mu(v_A - v_M) \left[ \frac{1}{\left[\frac{x^2}{r} + \frac{l}{E}p - 2h_0\right]^2} - \frac{q/\frac{1}{2}(v_A - v_M)}{\left[\frac{x^2}{r} + \frac{l}{E}p - 2h_0\right]^3} \right] \quad (4)$$

18  
 19  
 20 As in this flow situation we have a fully flooded nip inlet and a loaded nip, the Reynolds  
 21 (1886) separation boundary conditions used for load bearings are most appropriate, viz.:

$$22 \quad p(x_i = -\infty) = 0 \quad \text{and} \quad p(x_{out}) = \frac{dp}{dx}(x_e) = 0 \quad (5)$$

23  
 24  
 25 Eq. (5) expresses that the inlet ( $x_i$ ) to the flow is far upstream and has zero pressure and the  
 26 flow exits at  $x_e$  with both the pressure and pressure gradient equal to zero. Surface tension  
 27 effects on flow rate are thus ignored here.

28 An appropriate dimensionless form of Eq. (4) can be obtained by scaling the pressure  
 29 forces with the elastic forces ( $\frac{E}{l}$  \* length scale) which are the dominant forces in this system. A  
 30 natural length scale for the film thickness is a gap width, here half the absolute value of the  
 31 negative gap set,  $h_0$ . However, in the limit of operation when the two rollers are just  
 32 touching, this gap is zero and in such a case we must choose  $r$  as the length scale as it is the  
 33 only alternative dimension available, apart from the nominal contact width  $\sqrt{rh_0}$  which also  
 34 cannot be used. Using upper-scripts 0 and - to refer to the zero and negative gap cases  
 35 respectively and subscript  $r$  and  $h_0$  to denote the non-dimensional length scale basis, we

1 obtain the following non-dimensional forms of the model Eq. (4) and corresponding  
 2 dimensionless variables:

3 Zero Gap Case:

$$4 \quad \frac{dP_r}{dX_r} = Es \left[ \frac{12}{H_r^2} - \frac{24\lambda^0}{H_r^3} \right] \quad ; \quad H_r = X_r^2 + P_r - 0 \quad (6)$$

$$5 \quad X_r = x/r \quad H_r = h/r \quad H_{A,r} = h_A/r \quad S = v_A/v_M \quad P_r = p/l^E r$$

$$6 \quad \lambda^0 = \frac{\frac{1}{2}q}{v_A[\frac{1-S}{2}]r} = \frac{1}{2}H_{A,r}/[\frac{1-S}{2}] \quad Es = \mu v_A[\frac{1-S}{2}]/[\frac{E}{l}(r^2)]$$

7

8 Negative Gap Case:

$$9 \quad \frac{dP_{h_0}}{dX_{h_0}} = Ne \left[ \frac{12}{H_{h_0}^2} - \frac{24\lambda^-}{H_{h_0}^3} \right] \quad ; \quad H_{h_0} = X_{h_0}^2 + P_{h_0} - 2 \quad (7)$$

$$10 \quad X_{h_0} = x/\sqrt{rh_0} \quad H_{h_0} = h/h_0 \quad H_{A,h_0} = h_A/h_0 \quad S = v_A/v_M \quad P_{h_0} = p/l^E h_0$$

$$11 \quad \lambda^- = \frac{\frac{1}{2}q}{v_A[\frac{1-S}{2}]h_0} = \frac{1}{2}H_{A,h_0}/[\frac{1-S}{2}] \quad Ne = \mu v_A[\frac{1-S}{2}]/[\frac{E}{l}(\frac{h_0^3}{\sqrt{rh_0}})]$$

12

13 The positive gap case can be derived similarly using  $+2h_0$  in place of  $-2h_0$  . For this  
 14 situation we label the corresponding flux as  $\lambda^+$  and we have the following result:

15

16 Positive Gap Case

$$17 \quad \frac{dP_{h_0}}{dX_{h_0}} = Ne \left[ \frac{12}{H_{h_0}^2} - \frac{24\lambda^+}{H_{h_0}^3} \right] \quad ; \quad H_{h_0} = X_{h_0}^2 + P_{h_0} + 2 \quad (8)$$

$$18 \quad X_{h_0} = x/\sqrt{rh_0} \quad H_{h_0} = h/h_0 \quad H_{A,h_0} = h_A/h_0 \quad S = v_A/v_M \quad P_{h_0} = p/l^E h_0$$

$$19 \quad \lambda^+ = \frac{\frac{1}{2}q}{v_A[\frac{1-S}{2}]h_0} = \frac{1}{2}H_{A,h_0}/[\frac{1-S}{2}] \quad Ne = \mu v_A[\frac{1-S}{2}]/[\frac{E}{l}(\frac{h_0^3}{\sqrt{rh_0}})]$$

20

21 For all situations, zero, negative and positive gap cases, the model equation expresses the  
 22 dimensionless flux,  $\lambda^0$  ,  $\lambda^-$  or  $\lambda^+$  , conveniently as a function of a single parameter, the  
 23 elasticity number  $Es$  in the case of zero gap and a gap scaled elasticity number  $Ne$  in the  
 24 negative or positive gap situations. These numbers are of course inter-related through the  
 25 non-dimensionalising length scales  $r$  and  $h_0$  as:

26

$$27 \quad \lambda^0 = \lambda^-(h_0/r) \text{ or } \lambda^+(h_0/r) \quad \text{and} \quad Ne = Es/(h_0/r)^{5/2} \quad (9)$$

28

29 The analysis presented thus far is typical of lubrication analyses of roll coating flows.  
 30 Indeed, except for the fact that we have a reverse roll situation, these equations are the same  
 31 as those used by many researchers for forward deformable roll coating (Coyle, 1988;  
 32 Carvalho and Scriven, 1997a, b; Carvalho, 2003; Gostling et al., 2003). As for solving these

1 equations, it is clear from the similarity of the equations, that the solutions, originally  
 2 obtained by Coyle (1988) for the *forward* situation should hold true here too- provided we  
 3 replace the average speed of the rollers in the forward mode by half the difference in speed in  
 4 the reverse case. Accordingly, the predictions obtained by Coyle (1988) for the forward case  
 5 were transformed (see Fig. 2) into the following two correlations for zero and negative gaps  
 6 respectively:

7  
 8 
$$\lambda^0 = 1.42 E_S^{0.44} \quad \text{and} \quad \lambda^- = 0.55 N e^{0.52} \quad (10)$$

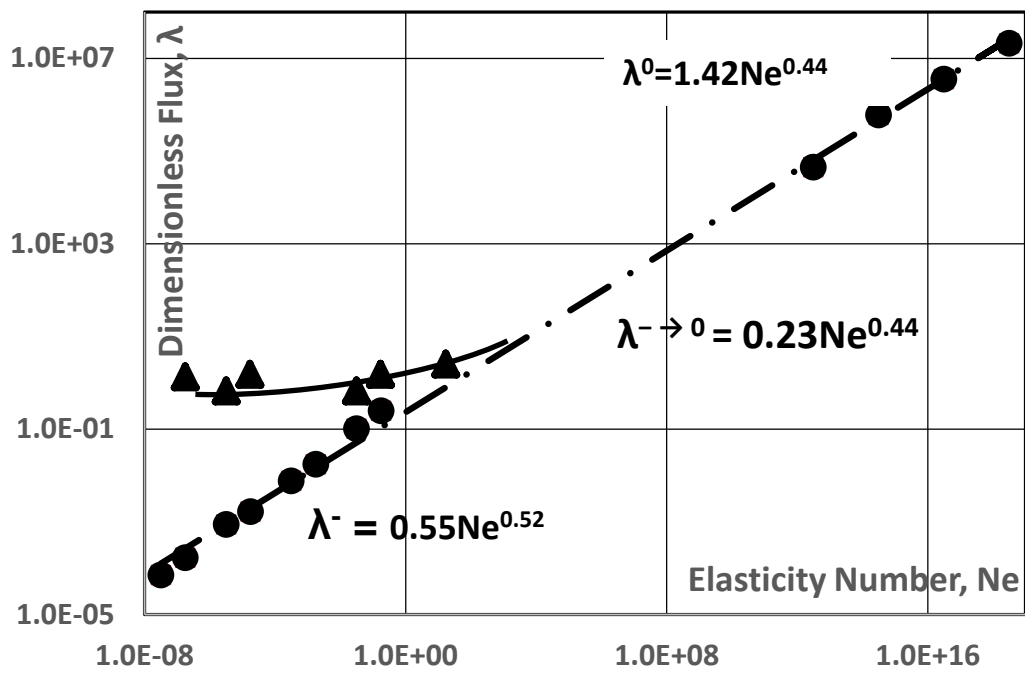
9  
 10 The above prediction for  $\lambda^-$  is a very close fit with the large deflection limit given by Coyle  
 11 (1988):

12  
 13 
$$\lambda^- = 0.40 N e^{0.50} \quad (11)$$

14  
 15 When we combine the two predictions for  $\lambda^-$  and  $\lambda^0$  in Eq. (10) in a single correlation  
 16 covering negative gap operation up to zero gap as in Fig. 2, we observe that they fit the  
 17 following equation:

18  
 19 
$$\lambda^{-\rightarrow 0} = 0.23 N e^{0.44} \quad (12)$$

20



21  
 22 **Fig. 2:** Predicted dimensionless flux as a function of elasticity number. Transformed from  
 23 Coyle (1988) original results (his Fig.6) for forward roll coating. (●: negative to zero gap, ▲:  
 24 zero gap to positive gap and to rigid system).

1  
2  
3  
4  
5  
6  
7  
8  
9  
10  
11  
12  
13  
14  
15  
16  
17  
18  
19  
20  
21  
22  
23  
24  
25  
26  
27  
28  
29  
30  
31  
32  
33  
34  
35  
36  
37  
38  
39  
40  
41  
42  
43  
44  
45

Eq. (10)-(12) as plotted in Fig.2 express that a decreasing  $Ne$  corresponds to an increasing negative gap (in absolute values) with the limit  $Ne \rightarrow \infty$  corresponding to the zero gap situation. In order to complete the analysis, we have also included in Fig.2 the results for positive reverse deformable roll coating. For this case increasing  $Ne$  corresponds to decreasing the positive gap with the limit  $Ne \rightarrow \infty$  corresponding also to the zero gap situation approached from high gaps. The limit  $Ne \rightarrow 0$  signifies a move into the rigid rollers regime where the set positive gap  $+2h_0$  only controls the film thickness as:

$$\lambda^+(Ne \rightarrow 0) = \frac{\frac{1}{2}q}{v_A[\frac{1-S}{2}]h_0} = \frac{1}{2}H_A h_0 / \left[\frac{1-S}{2}\right] = 4/3 \quad (13)$$

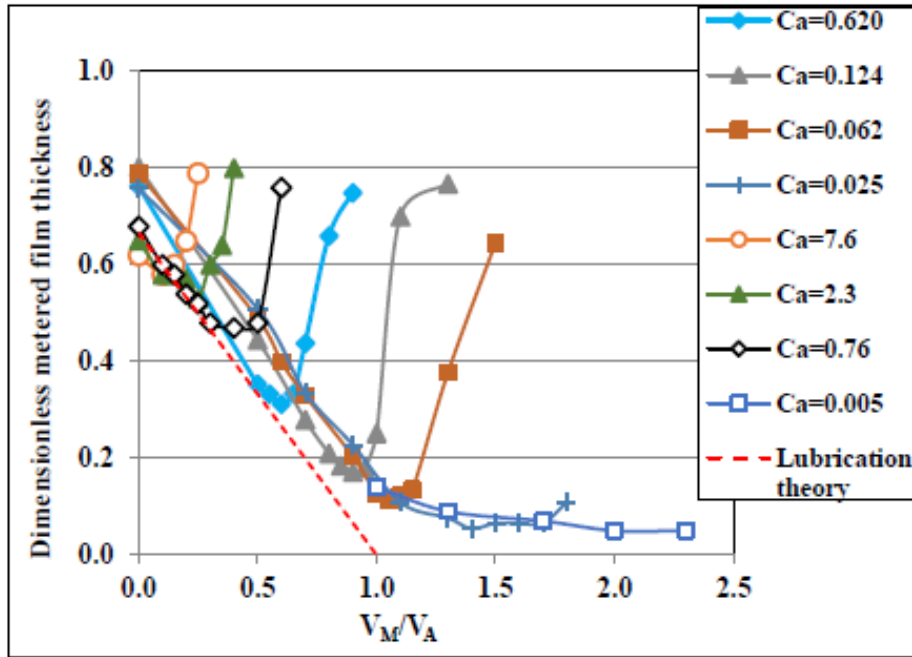
Eq. (13) is the classical result for rigid reverse roll coating, predicted by the lubrication approximation analysis and conforming to experimental data (Benkreira et al., 1981). Note also that Eq.(12) will of course also hold for forward roll coating when we replace  $-S$  by  $+S$ .

In the context of our present work, Eq. (12) is a useful theoretical guide which we will test against experimental data. Within the assumptions of the lubrication approximation, the above analysis and predictions are perfectly valid. However, whereas in negative deformable forward roll coating, the flow is more compliant with the lubrication approximation, with negative deformable reverse roll coating, it is less so as it is increasingly re-circulatory as the speed ratio is increased. This is particularly true at the inlet of the flow and more so at zero gap when the elasto-hydrodynamic coating length is narrow spanning very near the rollers dry contact point. At negative gaps, the rubber roller is pressed hard against the rigid roller resulting in the rollers surfaces being almost parallel with a comparatively longer nip region. Moreover, unlike in forward roll coating, in reverse roll coating the dynamic wetting line position, which will depend on the speed ratio is critical in film formation. Taking into consideration these limitations, it is expected that the constants and exponents in Eqs. (12) will not follow exactly the actual data, more so as  $S$  is increased and with the zero gap case.

Another important remark to add is that when a full analysis of rigid (i.e. positive, non-deformable gap) reverse roll coating is considered, an upturn in flow rates as the speed ratio is increased is predicted rather than the continuous linear decrease given by the lubrication approximation analysis (see Fig. 3). Such a behaviour is attributed to the penetration of the wetting line inside the gap as the speed ratio is increased, the trigger to what is known as “cascade”, “herringbones” or “seashores” instabilities which manifest themselves as cross-web bands of air (Coyle et al., 1990; Benkreira et al., 2013)). Figure 3 shows this clearly and explains why it is only by reducing the capillary number  $Ca$ , i.e. using very low viscosity fluids that one can push  $S^*$  (the critical speed ratio above which the upturn in flow rate occurs) to higher values, avoid the onset of cascade instabilities and obtain smaller film thickness. The question is: as the migration of the dynamic wetting line into the nip and the subsequent cascade instabilities are unlikely to occur with negative gap deformable roll coating because of the imposed load preventing the wetting line from moving into the gap (except may be at zero gap and with a very soft rubber), could we decrease the film thickness infinitely by increasing the speed ratio in negative gap operations? This is one critical aspect examined in this paper. But what of ribbing instabilities which are so common with roll coating flows? Interestingly, Benkreira et al. (2013) in the same work observed that

1 in rigid reverse roll coating with very low viscosity coating fluids, ribbing instabilities which  
 2 have the propensity to occur with increasing speed as the metering gap is reduced  
 3 disappeared instead as the metering gap was reduced. Typically, Benkreira et al. (2013) data  
 4 showed that with a coating liquid of viscosity 7mPa.s, stable films of thickness  $h_A = 7.5$   
 5 microns can be made at applicator speed  $v_A$  up to 1.5m/s when the positive gap  $+2h_0$  is set to  
 6  $25\mu\text{m}$ , the lowest permissible gap in their rigid reverse roll coating arrangement. So what if  
 7 the gap was reduced further using negative gap deformable roll coating, would we be able to  
 8 get even thinner films that are also free of ribbing? This is a second aspect, critical to flow  
 9 uniformity, to be examined in this paper.

10



11

12 **Fig. 3:** The upturn in film thickness with speed ratio in rigid reverse roll coating.. Data from  
 13 Benkreira et al., 2013 ( $Ca \leq 0.620$ ) and Coyle et al., 1990 ( $Ca \geq 0.76$ ).

14 In conclusion, the aim of this investigation is to assess the feasibility of negative gap  
 15 deformable reverse roll coating to produce very thin films at high speeds devoid of the  
 16 common cascade and ribbing instabilities observed in rigid roll coating. We have provided  
 17 above an analytical basis to guide us in identifying the key control parameters, namely the  
 18 elasticity number and make a comparison with the rigid roll coating situation. The motivation  
 19 is to extent further this very simple roll to roll liquid film coating method to produce very thin  
 20 films nearing a few microns for applications in the new technologies of plastic electronics,  
 21 organic photovoltaics, organic electronic devices, polymer electrolyte membrane fuel cells,  
 22 optical films for liquid crystal display and other high value thin film products to replace the  
 23 more expensive vacuum coating based batch processes. It is noted that for applications  
 24 where the substrate is not flexible - glass for example, the coated film will be transferred to  
 25 the glass substrate using a transfer roller.

26

### 27 3. EXPERIMENTAL METHOD

#### 28 3.1 The Coater and Operating Procedure

1 The coater consisted of two rollers, one rigid, made out of steel and one deformable,  
2 made out of a steel core covered with a rubber sleeve. The rigid roller was 0.20 m long and  
3 0.20 m in diameter, chromed and polished to provide an accuracy in the roller radius less than  
4  $\pm 2.5 \mu\text{m}$  with a chrome finish of  $\pm 0.1 \mu\text{m}$ . The deformable roller was also 0.20m long and  
5 had a steel shell of 0.20m in diameter and a rubber sleeve 15mm thick. A nitrile based rubber  
6 material (30, 50 and 70 shore A hardness) was selected as it was found to be the most  
7 resistant to swelling and corrosion when immersed in the coating fluids. The eccentricity of  
8 the deformable rollers was less accurate at  $\pm 25\mu\text{m}$  because of the difficulty in machining  
9 rubber. These precision levels are however amongst the best achieved in the industry.

10 The two rollers were mounted vertically, one on top of the other, slotted and held in  
11 place in a stiff stainless steel frame in which the gap could be changed and controlled  
12 accurately using spring loaded bearing blocks moved by a bolt, one on each side of the frame.  
13 The arrangement is shown schematically in Fig. 4.



15  
16 **Fig. 4:** Photograph of the experimental set-up.

17 As the operation investigated is concerned with negative gaps, it was necessary first to  
18 establish the zero position when the steel applicator roller and the metering deformable roller  
19 were just touching. This was achieved by shining a light beam between the rollers, moving  
20 the deformable roller towards the steel roller until the light just disappeared at which point  
21 the rollers were deemed to be just touching and the gap was zero. As the deformable roller  
22 had an eccentricity accurate to  $\pm 25\mu\text{m}$ , this zeroing procedure was performed at six positions  
23 across the length of the deformable roller. The gap at which the light was not seen at three  
24 points and seen at the other three points was taken to be the zero gap. The negative coating

1 gaps to be tested were then set by placing shims (Feeler Stock 667/Starrett) accurate to  $\pm$   
2  $0.1\mu\text{m}$  between the rollers bearing blocks. Gaps in the range of 0 to  $-200\mu\text{m}$  in steps of  $50\mu\text{m}$   
3 were tested.

4 With regard to the drive of the rollers, two inverter-controlled AC geared motors were  
5 used, one for each roller, in combination with timing pulleys and belts. The inverters were  
6 calibrated to provide  $\pm 0.1$  m/min accuracy in the control of the roller speeds. Feeding of the  
7 flow was organised by having the applicator roller partially immersed in a tank containing the  
8 coating liquid and doctoring the film picked up using a gapped steel rod attached to a vernier.  
9 Therefore, during the experiments, we could investigate the effect of feeding conditions from  
10 starved feeding to overfeeding (deemed to occur when a recirculating pool formed at the  
11 entrance of the nip). Note that following actual industrial operation and in order to replicate  
12 the theoretical flow situation depicted in Fig. 1, the film picked up by the metering roller was  
13 scrapped off to provide as dry a dynamic wetting line as possible. As a result, throughout the  
14 experiments, the liquid level in the feeder tank was maintained constant by a continuous  
15 topping up of fresh liquid.

16 The measurement of the metered film thickness was carried out by scraping the film  
17 off the applicator roller and weighting it. Experimental errors were reduced by carrying out  
18 the scraping over reasonably long periods of time, between 30 to 120 seconds, repeating the  
19 measurements and averaging the results. This gave an accuracy in the film thickness of  $\pm 3\%$ .

20 The onset of ribbing and cascade instabilities was observed under a strong but cold light  
21 to prevent any heating of the coating fluid, ramping up and down the rollers speed to within  
22  $0.2$  m/min of the critical condition.

### 23 24 **3.2 Design of Experiments**

25 As explained earlier in the Introduction, the aim of this study is to assess to what  
26 extent the film thickness can be reduced using negative gaps and remain stable. Clearly, in  
27 addition to large negative gaps and high speed ratios (up to 1 or greater if possible), low  
28 viscosity fluids are also required to produce very thin films as these conditions would reduce  
29 the hydrodynamic force opposing the large elastic deformation imposed. Hence our choice  
30 here of viscosities in the lower range, 10-200 mPa.s. Four such coating fluids were tested,  
31 three lubricating oils and one water-glycerine to ensure variation in surface tension was  
32 considered. The surface tensions were measured using the FTA 188 video tension meter the  
33 principle of which is to capture images of drops pending from a syringe to enable calculation  
34 of their diameter, volume thus weight and deriving surface tension from a force balance.  
35 Viscosities were measured using a classical cone and rotating plate shear flow instrument,  
36 here a Physica MCR 301, Anton Paar rheometer operated over a range of shear rates, 0-1500  
37  $\text{s}^{-1}$  to test that the fluids were indeed Newtonian. The measured viscosities at  $20^\circ\text{C}$  of the  
38 three lubricating oils were 7, 30 and 180 mPa.s and 6 mPa.s for the glycerine solution. The  
39 corresponding measured surface tensions were 26.8, 28.2, 28.6 and 65.4 mN/m.

40 Now, the deformation of the rubber is critical to the analysis presented above as an  
41 appropriate elastic modulus,  $E$  is required. In the roll coating situation described here, the  
42 rubber sleeve undergoes a cyclic deformation so an instrument capable of replicating such  
43 deformation is required. In this regard, the elastic modulus was measured using a dynamic  
44 mechanical analyser (Q800DMA, TA Instruments) according to the ASTM standard D4065  
45 where a small deformation was applied to a sample in a cyclic manner. Effectively, the DMA  
46 measures visco-elastic properties, namely the storage modulus  $E'$  and the loss modulus  $E''$   
47 (expressed by the loss factor,  $\tan(\alpha) = E'/E''$ ) as a function of deformation frequency,  $f_d$ .  
48 Fig.5 gives the pertinent data for the three rubbers, showing that the storage modulus varies  
49 with frequency. A choice of two moduli are available to approximate  $E$ : the storage modulus

1  $E'$  or the absolute value of complex modulus  $|E^*|$  given by  
 2 (<http://www.tainstruments.com/q800/>):

$$3 \quad |E^*| = E' \sqrt{1 + \{\tan(\alpha)\}^2} \quad (14)$$

5 As the loss factor  $\tan(\alpha)$  measured is small (was found to vary between 0.15 and 0.40 in  
 6 the range of frequency measured), the above equation reduces to:

$$7 \quad |E^*| \approx E' \quad (15)$$

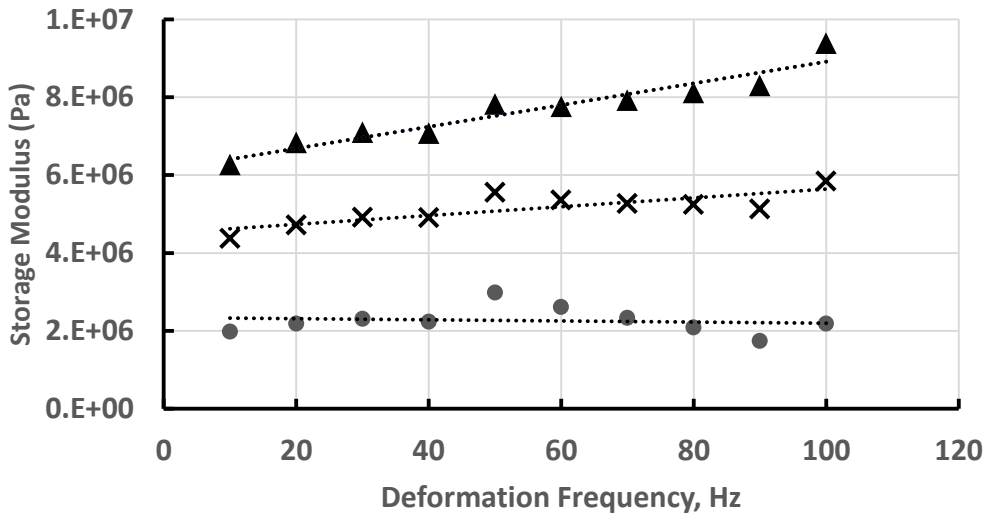
8 In other words, the DMA characterisation has revealed that over the frequency measured (up  
 9 to 100Hz), the rubber deforms essentially elastically and the storage modulus  $E'$  is indeed a  
 10 good approximation of the elastic modulus. There is however the necessity to assign a value  
 11 for the modulus of each of the rubbers used at the appropriate frequency of the coater. If the  
 12 deformation contact length between the two rollers is  $c_l$  and the rotational speed of the  
 13 deformable roller is  $v_M$  then the deformation frequency will be:

$$15 \quad f_d = v_M / c_l \quad (16)$$

17 An estimate of the contact length can be obtained by considering the static situation, which  
 18 from geometry gives:

$$19 \quad c_l = 2\sqrt{r^2 - (r - h_0)^2} \approx 2\sqrt{2rh_0} \quad (17)$$

21 Using these equations, we are now able to extract from Fig.5 the *dynamic* modulus.  
 22 By dynamic modulus, we mean the modulus at the frequency experienced by the rubber  
 23 sleeve in the coater.



24  
 25 **Fig. 5:** Storage modulus of rubbers used with frequency measured with a dynamic  
 26 mechanical analyser (Shore Hardness 70A (▲), 50A (X) and 30A (●)).

27 Interestingly, the softer rubber of shore hardness 30A displays essentially a constant  
 28 elastic modulus in the range of frequency tested. This makes it convenient to assess the  
 29 validity of the lubrication model described above. The other two rubbers and the hardest  
 30 rubber in particular (70A) show a non-negligible variation of the modulus with frequency.  
 31 This variation is shown to be linear in the range of frequency measured. As the contact length

1 is very small (order mm) and the speed large (order m/s), the deformation frequency will be  
2 generally large (order 1000 s<sup>-1</sup>) so the changes in  $E$  will be significant. Typically, the hard  
3 rubber will have  $E=6$  MPa at low frequencies (metering speed) going to 17 MPa when the  
4 metering speed is 150 m/min and the gap 100  $\mu\text{m}$ .

5 An important note is the large error that can be made by inferring a value for  $E$  from  
6 shore hardness values using semi-empirical correlations such as those often quoted in the  
7 literature. For example, Gent (1958) correlation which is widely used, gives:

$$8 \quad E = \frac{0.0981(56+7.66*Shore\ Hardness)}{0.137505(254-2.54*Shore\ Hardness)} \quad (18)$$

9 The elastic modulus predicted from Eq. (18) differs significantly (by a factor of 2) from the  
10 modulus measured as given in Fig. 5.

## 12 **4. RESULTS AND DISCUSSION**

13 The data are given in two forms, first dimensionally to assess how thin, fast and stable  
14 the films in this novel coating technique can be produced. Such dimensional presentation is  
15 important to assess feasibility for industrial applications. A second presentation, in  
16 dimensionless form, is also given to underpin the theoretical considerations described above  
17 and future more comprehensive analyses.

### 18 **4.1 Dimensional Film Thickness & Stability Window: Negative Gap**

19 A typical data set is given in Fig.6 which show the film thickness as a function of  
20 applicator roller speed  $v_A$  and speed ratio  $S$  in the range 30-150 m/min and 0-1 respectively  
21 for the three lubricating oils tested at the negative of -100  $\mu\text{m}$  with the hardest rubber of shore  
22 hardness 70A. The key and industrially favorable information from this data is that with  
23 negative gap operation we could increase coating speed and decrease film thickness  
24 *continuously* towards 0  $\mu\text{m}$  (no upturn as in Fig.3) without observing any of the cascade  
25 instabilities common with rigid reverse roll coating. This behavior was observed for all the  
26 negative gaps tested [-50  $\mu\text{m}$ , -100  $\mu\text{m}$ , -200  $\mu\text{m}$  and -300  $\mu\text{m}$ ] at all coating fluid viscosities  
27 [7 mPa.s, 30 mPa.s and 180 mPa.s] and rubber Shore hardness [30A, 50A and 70A] as shown  
28 in Figs.7 and 8. The hypothesis made earlier that pressing the rubber roller against the rigid  
29 roller prevented the movement of the dynamic wetting line inside the nip and the onset of  
30 cascade instabilities is thus verified. Furthermore, with regard to stability to ribbing, the data  
31 collected show that unlike with rigid roll coating, in deformable roll coating the coating  
32 window is widened over a larger range of speed ratios as the applicator roller speed and/or  
33 viscosity is increased (see Fig.6) and/or negative gap increased (see Figs.8a,b). This  
34 observation is in agreement with the data reported in an earlier paper by Benkreira et al.  
35 (2013) on rigid reverse roll coating with very low viscosity fluids.

### 36 **4.2 Dimensional Film Thickness & Stability Window: Zero Gap**

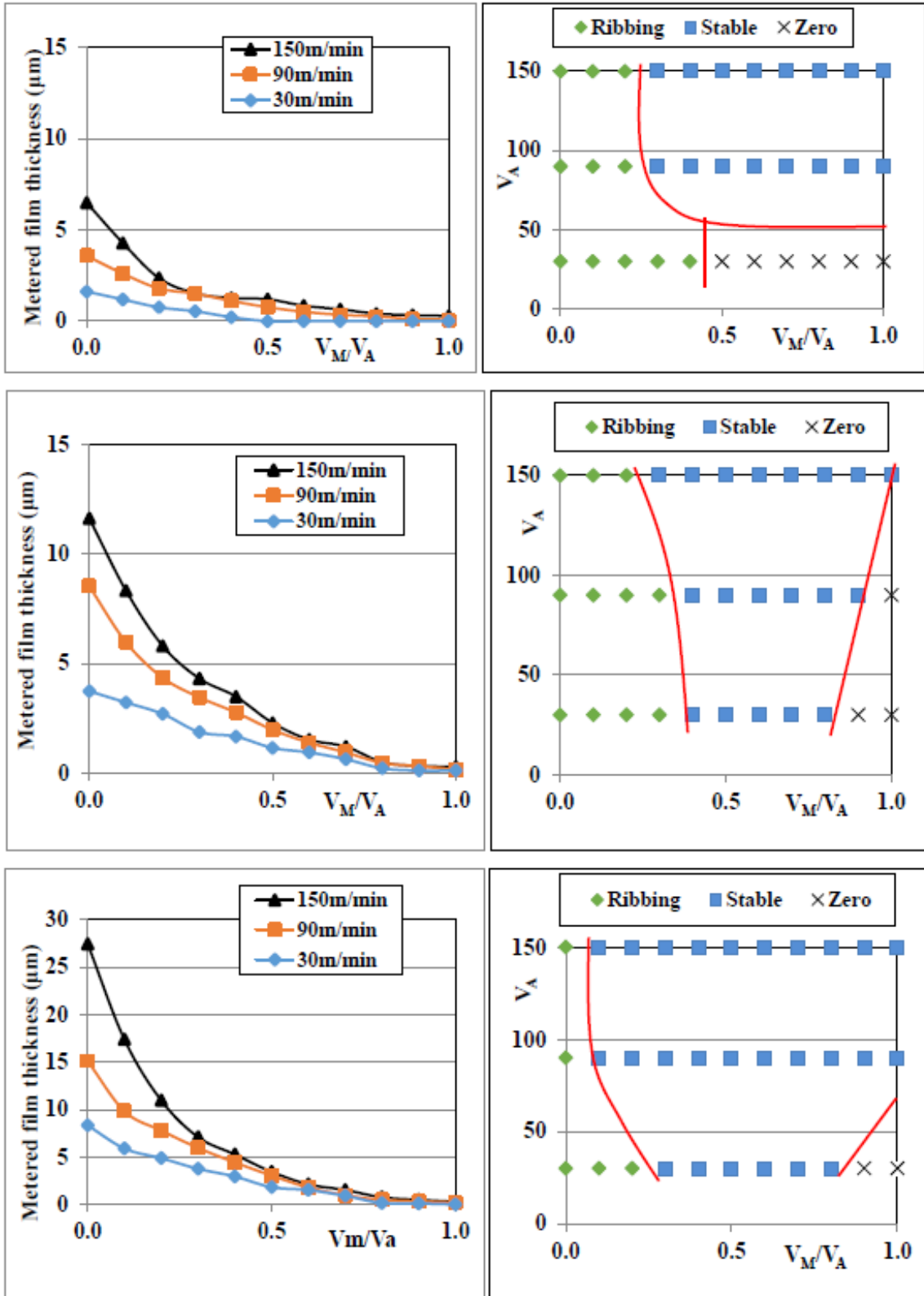
37 Fig. 9 present the zero gap data with the softest rubber (Shore Hardness 30) and  
38 lowest fluid viscosity (7 mPa.s) in a wide range of speeds [30 to 150 m/min] and speed ratios  
39 [0 to 1]. Using the softest rubber at zero gap approaches the rigid roll coating conditions as it  
40 allows the metering gap to open up positively and the dynamic wetting line to move into the  
41 nip as the speed ratio is increased. Interestingly the data reveal the occurrence of cascade  
42 instabilities and an up-turn in film thickness at a critical speed ratio just as observed in rigid  
43 roll coating. This data demonstrates a continuity in the flow behaviour of reverse roll coating  
44 in that cascade instabilities are indeed a fundamental feature associated with the migration of  
45 the dynamic wetting line into the nip and preventable only upon the application of a negative

1 gap. As for stability to ribbing, the behavior is similar to negative gap in that there is a  
2 minimum speed ratio ( $\approx 0.5-0.6$ ) below which the flow is unstable. These ribbing instabilities  
3 together with the cascade instabilities narrow stable operation at zero gap to a very small  
4 range of speed ratios as can be seen in Figs.8a, b and 9a, b.

5

6

7



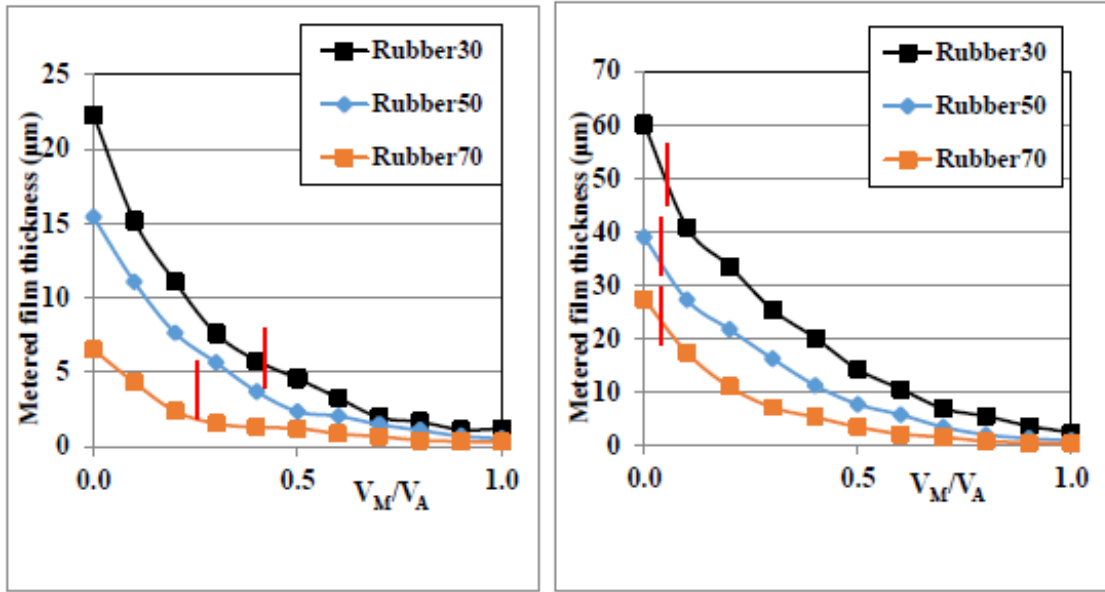
1

2

3

4

**Fig. 6:** Film thickness & stability window measured with the hardest rubber of **shore 70A** at - **100 μm gap** with fluids of viscosity **7, 30 and 180 mPa.s** respectively.



(a): -100  $\mu\text{m}$  and 7 mPa.s

(b): -100  $\mu\text{m}$  and 180 mPa.s

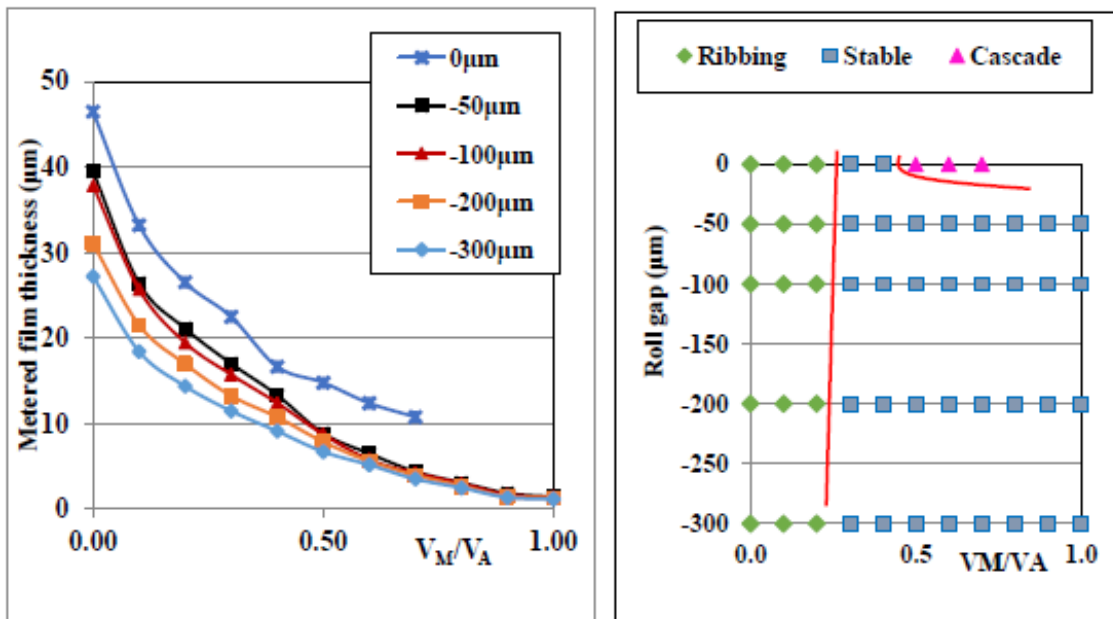
1

2

**Fig. 7:** Film thickness & stable speed ratio at high speed operation  $V_A=150$  m/min with various rubber hardness at low and high viscosity and gap of -100  $\mu\text{m}$ .

3

4



5

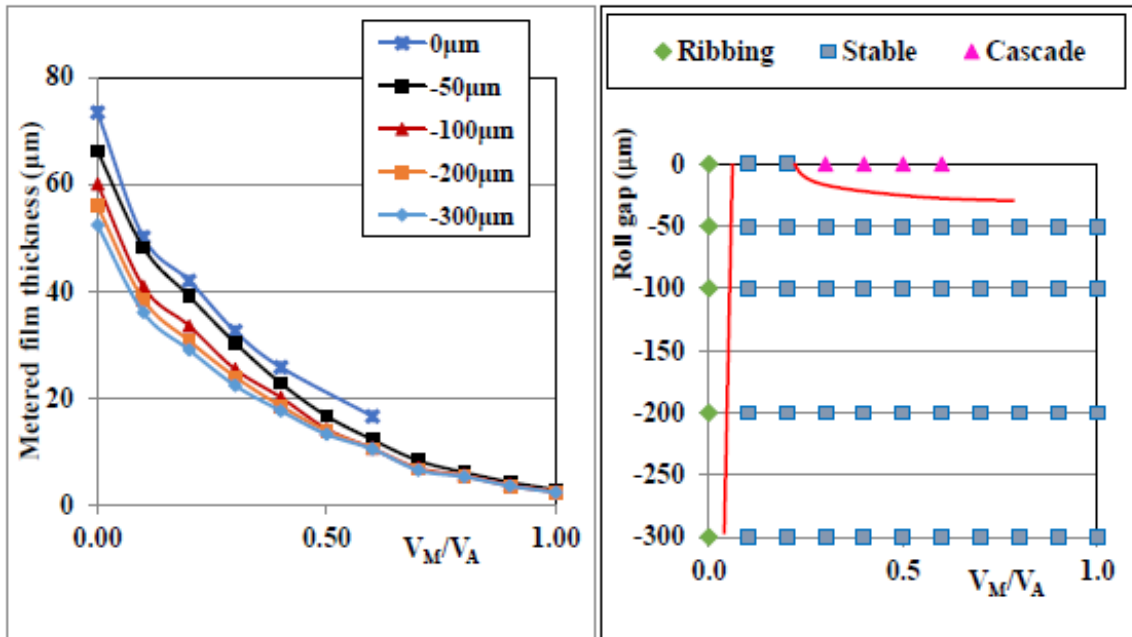
6

**Fig. 8a:** Film thickness & stability window at high speed ( $V_A=150$  m/min) with the soft rubber (30A) at low (30 mPa.s) viscosity and gap=0 and below

7

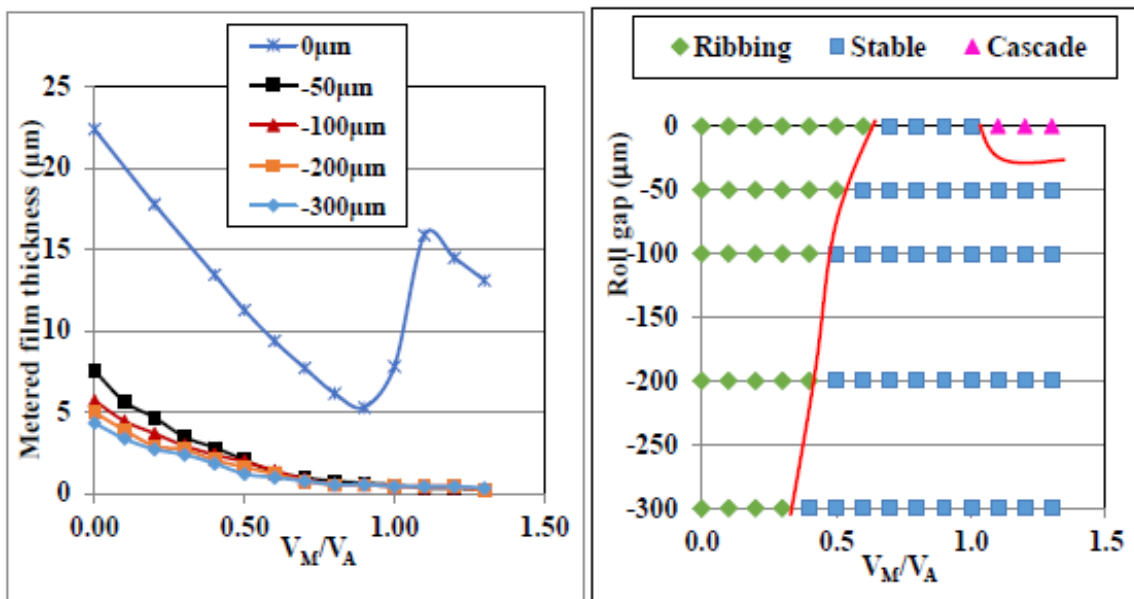
8

9



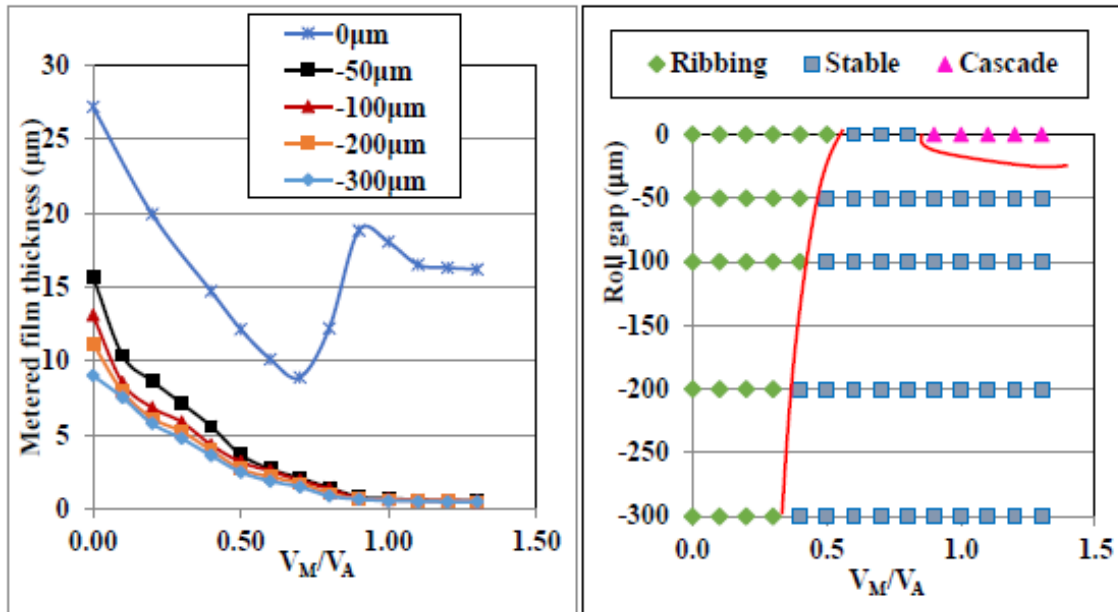
1  
2  
3  
4

**Fig. 8b:** Film thickness & stability window at high speed ( $V_A=150$  m/min) with the soft rubber (30A) at high (180 mPa.s) viscosity and gap=0 and below



5  
6  
7  
8  
9  
10

**Figure 9a:** Data demonstrating that cascade instability is a feature of reverse roll coating preventable only by application of a negative gap. Conditions here are: softest rubber (30A), lowest viscosity (5 mPa.s) and  $V_A=30$  m/min.



1

2

**Fig. 9b:** Data demonstrating that cascade instability is a feature of reverse roll coating preventable only by application of a negative gap. Conditions here are: softest rubber (30A), lowest viscosity (5 mPa.s) and  $V_A = 90$  m/min.

4

### 4.3 Dimensional Thickness & Stability Window: Comparison with Rigid Roll Coating

7

Fig.10a, b, c provides a comparison of the film thicknesses measured with a rigid steel roller at positive gaps between +25 μm and +100 μm and the softest rubber (30A shore hardness) at gaps ranging from +100 μm down to -300 μm. The data cover a wide range of operating conditions, fluid viscosities from 7 to 180 mPa.s and coating (applicator roller) speeds from 30 to 150m/min. The comparison is made at the lowest obtainable film thickness in rigid reverse roll coating, i.e. at the critical (highest) speed ratio  $S^*$  just before cascade instabilities are triggered. For example, (Fig. 10a), for operation at  $V_A = 30$  m/min, cascade instabilities were found to occur in rigid roller operation at  $S^* = 0.3, 0.6$  and  $0.9$  when the viscosity fluid was 180, 30 and 7 mPa.s respectively. The benefit of using a deformable negative gap are clear to see as the film thickness can be decreased comparatively further, down to nearly zero. Interestingly, whereas with the classical positive gap, the decrease is almost linear, i.e. steep, with the deformable negative gap, the decrease is flatter. The implication is that whereas small gap changes in rigid reverse roll coating are reflected proportionally in the film thickness formed, with deformable reverse roll coating, they are not, the film thickness levels off as the negative gap is further decreased. This is important in practice as in industrial operations small variation in the gap set will occur.

23

### 4.4 Dimensional Film Thickness & Stability Window: Operating Guide

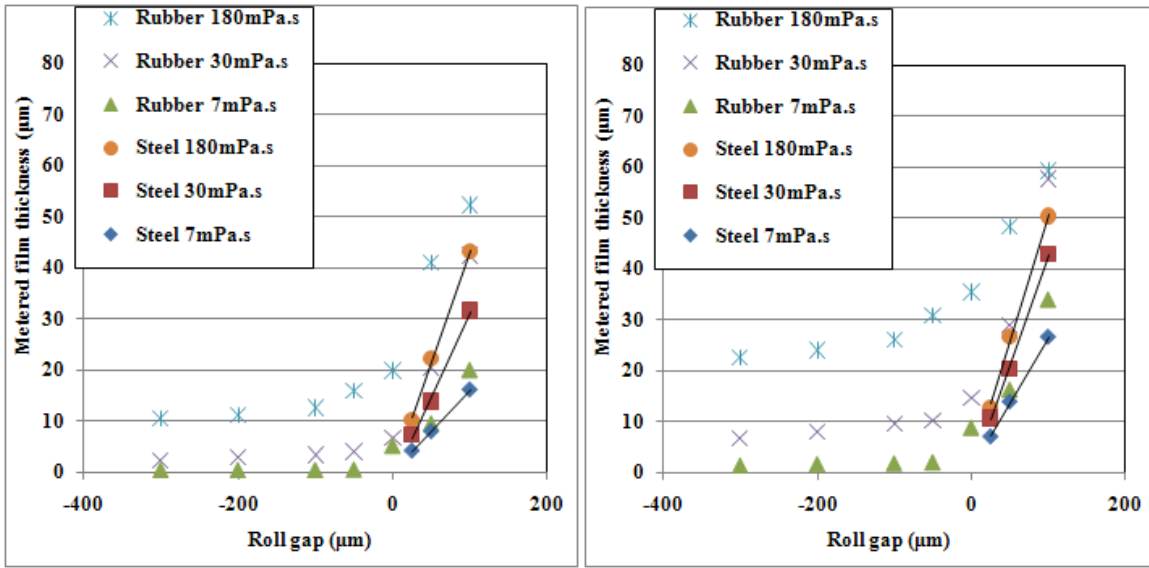
24

The data just presented indicate that deformable reverse roll coating is a very effective technique in that stable films of very low thickness can be achieved at high speeds with liquids in the viscosity and rubber hardness range tested (7-180 mPa.s and 30-70 Shore A). Moreover, the film thickness sensitivity to gap is very much reduced. Table 1, an operating guide for this coating method, summarizes the range of film thickness that can be achieved [1- 40 μm] at a coating speed range up to 150m/min. This is a remarkable achievement for

29

1 such a simple coating method, out-performing all other coating techniques, including slot  
 2 coating (see Benkreira and Ikin, 2016; Lee et al., 1992).

3

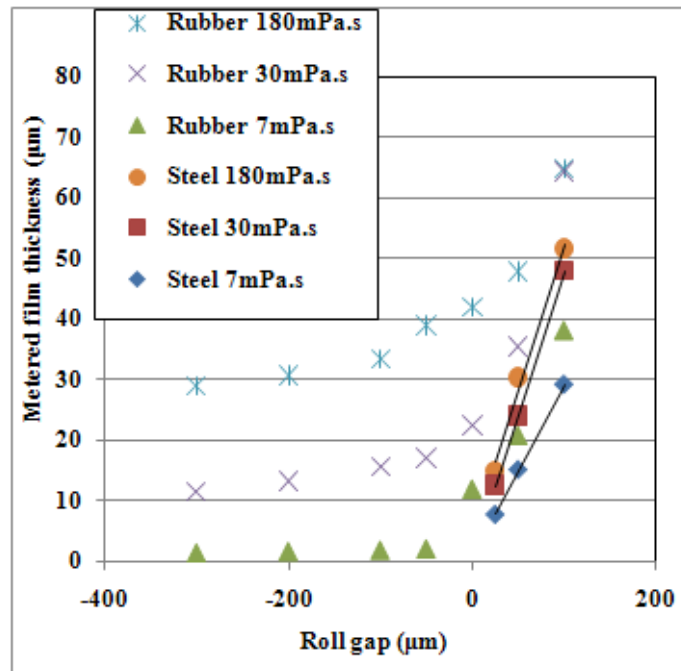


4

5

(a)  $V_A = 30\text{m/min}$

(b)  $V_A = 90\text{m/min}$



6

7

(c)  $V_A = 150\text{m/min}$

8 **Fig.10:** Dimensional Film Thickness & Stability Window: Comparison of 30A shore  
 9 hardness with Rigid Roll Coating at critical speed ratio  $S^*$ . (a):  $S^* = 0.3$  (180 mPa.s), 0.6 (30

10 mPa.s) and 0.9 (7 mPa.s); (b):  $S^* = 0.2$  (180 mPa.s), 0.4 (30 mPa.s) and 0.7 (7 mPa.s); (c):

11  $S^* = 0.2$  (180 mPa.s), 0.3 (30 mPa.s) and 0.7 (7 mPa.s).

1

2 **Table 1:** An operating guide showing the range of stable film thickness and speed achievable  
 3 in deformable reverse roll coating.

Gap: minus 100 $\mu$ m

Rubber	Viscosity (mPa.s)	LS (m/min)	Min. ( $\mu$ m)	Max. ( $\mu$ m)
70	7	30	-	-
		90	0.3	1.5
		150	0.3	1.5
	30	30	0.2	1.7
		90	0.3	2.8
		150	0.3	4.3
	180	30	0.2	3.8
		90	0.2	9.8
		150	0.3	17.4
50	7	30	0.2	1.3
		90	0.4	2
		150	0.5	2.3
	30	30	0.3	2.3
		90	0.6	5.9
		150	0.6	9.7
	180	30	0.7	6.5
		90	0.7	17.9
		150	0.9	27.3
30	7	30	0.2	2
		90	0.5	3.2
		150	1.2	4.6
	30	30	0.9	3.4
		90	1.2	9.5
		150	1.5	15.7
	180	30	1.2	12.6
		90	1.5	26.1
		150	2.4	40.9
	7*	30	0.2	1.9
		90	0.4	4.5
		150	0.9	8.8

7\*: The surface tension is 65mN/m.

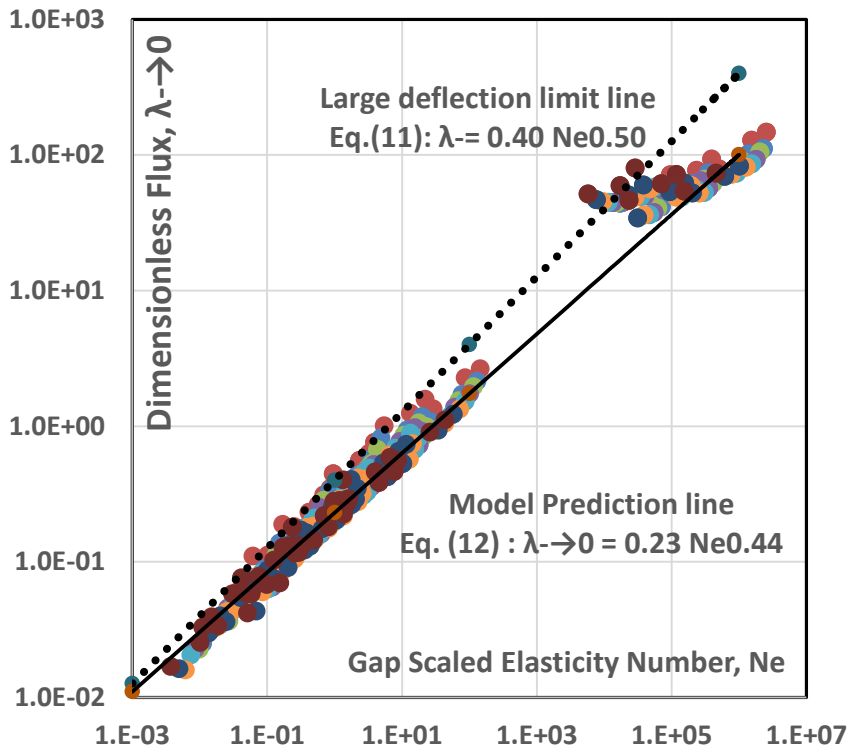
4

#### 5 4.5 Dimensionless Film Thickness

6 Here we test the validity of the theoretical lubrication approximation predictions  
 7 presented earlier in Eq. (12) against the data collected. Fig.11 gives such a presentation for  
 8 data collected with the softest rubber of shore hardness 30A at gaps 0, -50, -100, -200 and -  
 9 300 $\mu$ m, with all the four fluids at speed ratio up to 0.7. Recall that this rubber was the one

1 that exhibited an elastic modulus value (see Fig.5) that was independent of deformation  
 2 frequency. It is thus well suited to comparison with the model predictions.

3



4

5 **Fig. 11:** Comparison between measured film thicknesses and lubrication approximation  
 6 predictions. Softest rubber 30A, all gaps, all fluids, speed ratio 0 to 0.7.

7

8 A remarkably close fit with the lubrication approximation prediction is obtained with  
 9 the data correlating with a coefficient of determination  $R^2=0.99$  in the entire gap range as:

10

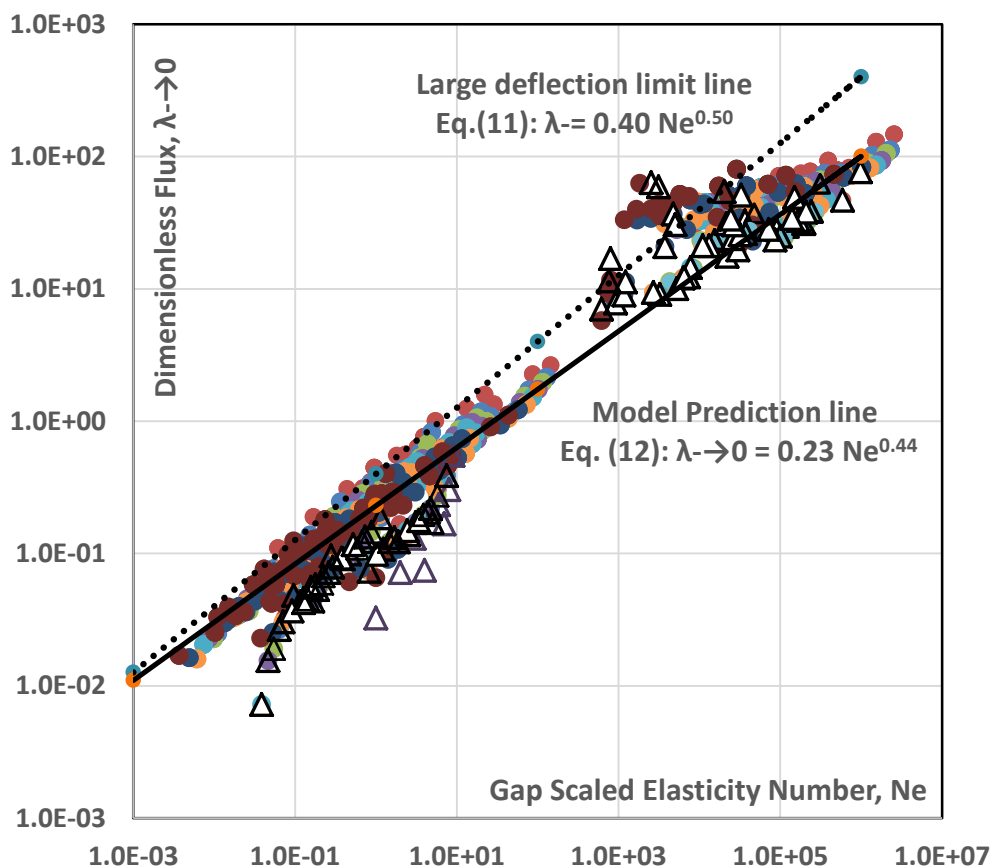
$$11 \quad \lambda^{-\rightarrow 0} = 0.25 Ne^{0.50} \quad (19)$$

12

13 At zero gap, the fit is less good which is to be expected as we are moving from a regime  
 14 where the elastic forces control of the gap diminishes to a regime where eventually (rigid  
 15 roller case) the gap (positive gap  $h_0$ ) only controls the film thickness. Note that applying the  
 16 principle of propagation of errors to Eq. (19), we estimate from the definition of  $Ne$  ( $=$   
 17  $\mu v_A \left[ \frac{1-S}{2} \right] / \left[ \frac{E}{l} \left( \frac{h_0^3}{\sqrt{r} h_0} \right) \right]$ ) and the errors in the various parameters  $\mu, v_A, v_B, E, l, r, h_0$  that the  
 18 error in the measured dimensionless flux is about 5% but only when  $E$  is measured with a  
 19 good degree of accuracy (better than 5%). Note also that both  $\lambda^{-\rightarrow 0}$  and  $Ne$  depends on  $h_0$   
 20 thus both Eq. (9) and (19) are required to calculate the actual film thickness  $h_A$ . If we take a  
 21 typical example of an elasticity number  $Es = 10^{-8}$ , we find for a typical dimensionless  
 22 negative applied gap  $h_0/r = 10^{-3}$  that the modified elasticity number given by Eq.(9) will  
 23 be  $Ne = 0.316$ . The corresponding dimensionless flux calculated from the best data fit Eq.  
 24 (19) is  $\lambda^{-\rightarrow 0} = 0.1405$  and from the theoretical prediction Eq. (12) is  $\lambda^{-\rightarrow 0} = 0.1385$  making

1 the error very small (1.4%). For typical conditions of a negative gap of 100 $\mu$ m, a roller radius  
 2 of 10cm and a speed ratio of 0.5, this translates to a film thickness  $h_A = 0.140 \times 10^{-3} \times$   
 3  $0.10 \times 0.5 = 7\mu$ m.  
 4  
 5

6 To test further the fit with the lubrication approximation prediction, Fig. 12 assembles  
 7 all the data, for the three rubbers at speed ratios 0 to 0.7 using the dynamic modulus (i.e. with  
 8 E values at the corresponding deformation frequency). Whereas the data with the rubber of  
 9 shore hardness 50A approach superimposition onto the data with the soft rubber, the harder  
 10 rubber of shore hardness 70A show significantly thinner films but only in the negative gap  
 11 region. As there is a good fit at zero gap, the data suggest that the elastic response of the hard  
 12 rubber depends on the extent of the initial deformation imposed. This is not captured in the  
 13 DMA where the sample is not preloaded. Note also that the linear variation of the modulus  
 14 with frequency shown in Fig.5 may not hold at frequency above those measured (0-100Hz).  
 15 During the actual coating operation, deformation frequencies in excess of 100Hz would occur  
 16 as metering speeds up to 150m/min were used. As pointed out by Carvalho (2003), the  
 17 thickness of the rubber sleeve as well as the viscoelastic properties should be considered in a  
 18 full analysis.  
 19



20  
 21 **Fig. 12:** Comparison between measured thickness and lubrication approximation predictions.  
 22 All three rubbers, all gaps, all fluids and speed ratio 0 to 0.7. ( $\Delta$ : Shore Hardness 70A).  
 23  
 24

## 1 5. CONCLUSIONS

2 Although roll coating is widely used in industry and has been the subject of  
3 numerous papers, this is the first study that describes the reverse roll coating operation with a  
4 negative gap using a deformable roller. The data presented here and obtained over a wide  
5 range of conditions, demonstrate that compared with positive gap operations, reverse roll  
6 coating operated with a deformable negative gap is capable of achieving much thinner  
7 uniform films as low as 1 micron. Also, the data reveal that whereas with the classical  
8 positive gap, the decrease is almost linear, i.e. steep, with the deformable negative gap, the  
9 decrease is flatter. The implication is that whereas small gap changes in rigid reverse roll  
10 coating are reflected proportionally in the film thickness formed, with deformable reverse roll  
11 coating, they are not, the film thickness levels off as the negative gap is further decreased.  
12 This is important in practice as in industrial operations variation in the gap will occur.  
13 Moreover, the data show that such flow is devoid of cascade instabilities which are inherent  
14 to positive gap operation because of the migration of the dynamic wetting line into the nip.  
15 The film formed are also free of ribbing instabilities over a wide range of speed when low  
16 viscosity fluids are used.

17 The dimensional data presented in this study can be used directly to inform industrial  
18 scale operation. As a first and good approximation, the entire data, from zero down into  
19 negative gap operation, can be represented by  $\lambda^{-\rightarrow 0} = 0.25Ne^{0.50}$  which gives the  
20 dimensionless flux through the nip as a simple function of a gap scaled elastic number,  $Ne$ .  
21 Clearly, more sophisticated models are desirable to further grab such features as the complex  
22 deformation of the rubber sleeve, the effect of the viscoelasticity of the rubber sleeve on the  
23 deformation and the two dimensional characteristics of the flow.

24

## 25 6. ACKNOWLEDGEMENTS

26 The authors acknowledge the support of the Films R&D Centre of Toyobo Co. Ltd.,  
27 Otsu, Japan and of the Thin Films Research Group of the University of Bradford, UK.

28

## 29 7. NOTATIONS

30	Ca	Capillary number [= $\mu v_A / \sigma$ ]
31	$c_l$	Rollers contact length [= $2\sqrt{2rh_N}$ ]
32	$E$	Rubber elastic modulus
33	$E'$	Rubber storage modulus
34	$E''$	Rubber loss modulus
35	$E^*$	Rubber complex modulus
36	$Es$	Zero gap elasticity number [= $\mu v_A [\frac{1-S}{2}] / [\frac{E}{l} (r^2)]$ ]
37	$f_d$	Rubber roller deformation frequency [= $v_M / c_l$ ]
38	$h$	Coating gap
39	$h_A$	Coating film thickness formed on applicator roller
40	$-2h_0$	Negative applied gap

1	$H_{h_0}$	Dimensionless gap with respect to the half the negative gap [= $h/h_0$ ]
2	$H_r$	Dimensionless gap with respect to the equivalent roller radius [= $h/r$ ]
3	$H_{A,h_0}$	Dimensionless film thickness with respect to half the negative gap [= $h_A/h_0$ ]
4	$H_{A,r}$	Dimensionless film thickness with respect to the equivalent roller radius [= $h_A/r$ ]
5	$l$	Thickness of rubber sleeve on metering roller
6	$Ne$	Gap scaled elasticity number [= $\mu v_A [\frac{1-S}{2}] / [\frac{E}{l} (\frac{h_0^3}{\sqrt{r h_0}})]$ ]
7	$q$	Coating flow rate
8	$p$	Pressure
9	$P_{h_0}$	Dimensionless pressure with respect to half the negative gap [= $p/\frac{E}{l} h_0$ ]
10	$P_r$	Dimensionless pressure with respect to the equivalent roller radius [= $p/\frac{E}{l} r$ ]
11	$r$	Equivalent radius of the two rollers [= $1/\{\frac{1}{2}(\frac{1}{r_A} + \frac{1}{r_M})\}$ ],
12	$r_A$	Applicator roller radius
13	$r_M$	Metering roller radius
14	$S$	Speed ratio [= $v_A/v_M$ ]
15	$S^*$	Critical speed ratio for onset of cascade instabilities
16	$v_A$	Applicator roller speed
17	$v_M$	Metering roller speed
18	$x$	Primary flow direction
19	$x_e$	Flow exit position
20	$x_i$	Flow inlet position
21	$X$	Dimensionless primary flow direction
22	$y$	Transverse flow direction
23	$Y$	Dimensionless transverse flow direction
24	$\lambda^-$	Dimensionless flow rate in negative gap operation [= $\frac{\frac{1}{2}q}{v_A[\frac{1-S}{2}]h_0} = \frac{1}{2}H_{A,h_0}/[\frac{1-S}{2}]$ ]
25	$\lambda^+$	Dimensionless flow rate in negative gap operation [= $\frac{\frac{1}{2}q}{v_A[\frac{1-S}{2}]h_0} = \frac{1}{2}H_{A,h_0}/[\frac{1-S}{2}]$ ]
26	$\lambda^0$	Dimensionless flow rate in zero gap operation [ $\lambda^0 = \frac{\frac{1}{2}q}{v_A[\frac{1-S}{2}]r} = \frac{1}{2}H_{A,r}/[\frac{1-S}{2}]$ ]
27	$\delta$	Rubber elastic deformation

- 1  $\mu$  Viscosity of coating liquid  
2  $\sigma$  Surface tension of coating liquid

3

#### 4 **7. REFERENCES**

- 5 Benkreira, H., Edwards, M.F., Wilkinson, W.L.,1981. Roll coating of purely viscous liquids.  
6 Chem. Eng. Sci. 36:429-434.
- 7 Benkreira, H., Edwards, M.F., Wilkinson, W.L.,1982. Ribbing instability in the roll coating  
8 of Newtonian fluids. Plastic Rubber Proc. Appl. 2, 137-144.
- 9 Benkreira, H., Ikin, J.B., 2016. Slot coating minimum film thickness in air and in rarefied  
10 helium. Chem. Eng. Sci. 150, 66-73.
- 11 Benkreira, H., Shibata, Y., Ito, K., 2013. Thinnest uniform liquid films formed at the highest  
12 speed with reverse roll coating. AIChE J. 59:3083-3091.
- 13 Carvalho, M.S. and L.E. Scriven, 1997, Deformable roll coating flows: Steady and linear  
14 perturbation analysis, J. Fluid Mech. 339, 143-172.
- 15 Carvalho, M., Scriven, L.E., 1997. Flows in forward deformable roll coating gaps:  
16 comparison between spring and plane-strain models of roll cover. J. Comp. Phys. 138, 449–  
17 479.
- 18 Carvalho, M.,2003. Effect of thickness and viscoelastic properties of roll cover on  
19 deformable roll coating flows. Chem. Eng Sci. 58, 4323 – 4333.
- 20 Coyle, D. J., 1988. Forward roll coating with deformable rolls: A simple one dimensional  
21 elastohydrodynamic model. Chem. Eng. Sci. 43, 2673–2684.
- 22 Coyle, D.J., 1997. Knife and Roll Coating. In: Kistler F, Schweizer PM. Liquid film coating.  
23 London: Chapman & Hall; 539-571.
- 24 Coyle, D.J., Macosko, C.W., Scriven, L.E.,1990. The fluid dynamics of reverse roll coating.  
25 AIChE J. 36(2), 61-174.
- 26 Gent, A.N., 1958. On the relation between indentation hardness and Young's modulus.  
27 International Rubber Institute Transactions 34, 46–57.
- 28 Gostling, M. J., Savage, M.D., Young, A.E., Gaskell, P.H., 2003. A Model for deformable  
29 roll coating with negative gaps and incompressible compliant layers. J. Fluid. Mech.  
30 489,155–184.
- 31 Grashof, B., Delgado, A.J., 2015. Analysis of influencing parameters in deformable roll  
32 coating of counter-rotating rolls. J. Coat. Technol. Res. 12, 63–73.
- 33 Pearson, J.R.A., 1960. The instability of uniform viscous flow under rollers and spreaders. J.  
34 Fluid Mech. 7, 481- 500.

1 Pitts, E., Greiller, J., 1961. The flow of thin liquid films between rollers. *J. Fluid Mech.* 11,  
2 33-51.

3 Lee, K.-Y., Liu, L.-D., Liu, T.-J., 1992. Minimum wet thickness in extrusion slot coating.  
4 *Chem. Eng. Sci.* 47, 1703–1713.

5 Reynolds, O., 1886. On the theory of lubrication and its application to Mr Beauchamp  
6 Tower's experiments including an experimental investigation of the viscosity of olive oil.  
7 *Phil. Trans. R. Soc. A* 177, 157-234.

8

9

10

11

12

13

14

15

16

17

18

19

20

21

22

23

24

25

26

27

28

29

1  
2  
3  
4  
5  
6  
7  
8  
9  
10  
11  
12  
13  
14  
15  
16  
17  
18  
19  
20  
21  
22  
23  
24  
25  
26  
27  
28  
29  
30  
31  
32  
33  
34

## LIST OF FIGURES

**Fig. 1:** Deformable reverse roll coating flow; geometry and pertinent parameters.

**Fig. 2:** Predicted dimensionless flux as a function of elasticity number. Transformed from Coyle (1988) original results (his Fig.6) for forward roll coating. (●: negative to zero gap, ▲: zero gap to positive gap and to rigid system).

**Fig. 3:** The upturn in film thickness with speed ratio in rigid reverse roll coating: Data from Benkreira et al., 2013 ( $Ca \leq 0.620$ ) and Coyle et al., 1990 ( $Ca \geq 0.76$ ).

**Fig. 4:** Photograph of the experimental set-up.

**Fig. 5:** Storage modulus of rubbers used with frequency measured with a dynamic mechanical analyser (Shore Hardness 70A (▲), 50A (X) and 30A (●)).

**Fig. 6:** Film thickness & stability window measured with the hardest rubber of shore 70A at -100  $\mu\text{m}$  gap with fluids of viscosity 7, 30 and 180 mPa.s respectively,  $V_A$  in m/min.

**Fig. 7:** Film thickness & stable speed ratio at high speed operation  $V_A=150$  m/min with various rubber hardness at low and high viscosity and gap of -100  $\mu\text{m}$ . RHS of vertical marker is stable region, LHS is ribbing.

**Fig. 8a:** Film thickness & stability window at high speed ( $V_A=150$  m/min) with the soft rubber (30A) at low (30 mPa.s) viscosity and gap=0 and below.

**Fig. 8b:** Film thickness & stability window at high speed ( $V_A=150$  m/min) with the soft rubber (30A) at high (180 mPa.s) viscosity and gap=0 and below.

**Figure 9a:** Data demonstrating that cascade instability is a feature of reverse roll coating preventable only by application of a negative gap. Conditions here are: softest rubber (30A), lowest viscosity (5 mPa.s) and  $V_A=30$  m/min.

**Fig. 9b:** Data demonstrating that cascade instability is a feature of reverse roll coating preventable only by application of a negative gap. Conditions here are: softest rubber (30A), lowest viscosity (5 mPa.s) and  $V_A=90$  m/min.

1

2

3

4

## LIST OF TABLES

5

6 **Table 1:** An operating guide showing the range of stable film thickness and speed achievable  
7 in deformable reverse roll coating.

8